Desalination and Water Treatment
www.deswater.com

doi: 10.5004/dwt.2017.20967

80 (2017) 326–336
June

Enhancement of synthetic zeolite (Crystal-Right) adsorption characteristics toward NH_4^+ by regeneration

Miroslav Kukučka[a], Nikoleta Kukučka Stojanović[a,*], Lucija Foglar[b]

[a]*EnviroTech d.o.o., Sterije Popovića 42, 23300 Kikinda, Serbia, Tel. +38163501908, +38163517528; Fax: +381 230 437 999; emails: nikol@envirotech.rs (N.K. Stojanović), miroslav@envirotech.rs (M. Kukučka)*
[b]*University of Zagreb, Faculty of Chemical Engineering and Technology, Marulićev trg 19, 10000 Zagreb, Croatia, Tel. +385915693837; email: lfoglar@fkit.hr*

Received 10 January 2017; Accepted 25 May 2017

ABSTRACT

Breakthrough (CC_{BTP}) and exhaustive column capacities (CC_{EP}) of synthetic zeolite (Crystal-Right [CR]) in original form and zeolite in several forms obtained after regeneration processes, toward ammonium was examined during subsequent NH_4^+ adsorption tests using different ratios of NaCl and NaClO for regeneration. The breakthrough point's calculations were used for dimensionless adsorption power coefficients (APC) establishment that indicated CC_{BTP} and CC_{EP} values, respectively. It was shown that H^+ increased as a consequence of NaClO hydrolysis in the presence of brine sodium cations, and its bonding to zeolite active sites significantly reflected on column capacity values. The bonding of generated protons to basic synthetic zeolite structure oxygen bridges enhanced the number of active sites suitable for NH_4^+ ion-exchange. This catalytic effect of NaClO to H^+ enabled iterative usage of synthetic zeolite for NH_4^+ adsorption with enhanced adsorption properties. Optimal molar ratio of regenerants quantity (R_{AT}) and exhaustive column capacity expressed in moles and defined as R_{AT}/CC_{EP} of 312.85 contributed to increase of column capacities with regard to the original zeolite. Adsorption processes G, H and I provided the highest specific APC breakthrough point of 0.81, 0.75 and 0.76 and APC exhausting point of 0.52, 0.54 and 0.53, respectively, which indicated better ammonia bonding onto those CR than the original CR and other regenerated CRs. Larger part of ammonia was bonded to CR crystalline structure by electrostatic adsorption and was successfully eliminated in strong oxidation process by NaClO in engaged regeneration modes (F–H). The best results of CR adsorption properties enhancement were obtained in regeneration modes (F–H), which were conducted using mixture of NaCl and NaClO in molar ratios of 10.62:1, 7.07:1 and 21.24:1, respectively. Ammonia removal efficiency was higher in three adsorption processes that were conducted with regenerated zeolite than removal efficiency obtained with native non-regenerated zeolite.

Keywords: Adsorption characteristics enhancement; Ammonia adsorption power coefficient; Regeneration; Synthetic zeolite; Breakthrough column capacity; Exhausting column capacity

1. Introduction

Natural and synthetic zeolites are highly porous zeolites that belong to structural class of ion-exchangeable systems and the diversity of zeolite crystals is a consequence of different crystal types especially expressed in wide range of Si/Al relations and Al distribution over the lattice as well [1]. Within the framework of zeolites cavities, it is evident that the amount of existing monovalent cations is twice the content of divalent cations. These phenomena are induced by the charge balance principle and explained on the base of cation-hopping polarization hypothesis [2]. It is known that aluminum distribution and zoning, especially spatial ones, within a zeolite crystal, is crucial for physicochemical characterization, catalytic performance and application of zeolites [3]. Zeolites characterize catalytic properties through Brønsted acid, Lewis acid and oxidation reaction active sites, so the zeolite surface acidity emphatically depends on the

* Corresponding author.

exchanged cation nature [4]. Zeolite protons in H^+ forms are coordinated to oxygen atoms and constituted OH groups [5] which showed a range of acid strength. Different wavelengths of present hydroxyl groups depend on Si/Al ratio and its position in framework cages is changing the zeolite nature from weak to strong acid sites. Investigated changes in hydroxyl groups wavelengths are actually related to decrease in interactions between $(AlO_4)^-$ tetrahedra, observed from the low to high Si/Al ratios [6]. Modifications in zeolite framework cation field are based on the increase in ionic strength and formation of new acid sites which results in the adsorption capacity enhancement. The polarization of hydroxyl groups produces more active protons, especially during the acid strength increase in polyvalent cationic zeolites [7]. At the base of zeolite hydration, upon water hydrolysis, the significant generation of protons is observed as charge interactions in framework [8]. When zeolite sodium cations are exchanged for protons, a linear increase in acid strength is indicated. The decrease in the framework interactions induced with Si/Al ratio rising, in the same time, increased activity coefficients. The enhancement of zeolites adsorption capacity by the increase of suitable active sites quantity was the scope of many investigations and the revitalization of zeolite pores filled with sorbate was achieved by action of specific chemicals–regenerants [9,10]. These chemicals either by ion-exchange or other physicochemical process like dissolution [11] or oxidation [12] are capable of restoring zeolite active sites and specific surface area to the same or better conditions as in the original material. Besides the chemicals, microbiological processes can also discharge zeolite pores [13]. Synthetic zeolites bond ammonium very efficiently, contrary to natural zeolites that also remove ammonium but only with one-fourth of the capacity of synthetic zeolites. Natural zeolites are also very ineffective with regard to regeneration. Synthetic zeolites such as Crystal-Right CR-100 and CR-200, remove ammonium with great efficiency and can be regenerated using only brine and Na-hypochlorite [14].

With appreciation to zeolite's molecular screen characteristics and their distinct capability toward ion-exchange, zeolites are more and more used as adsorbents in separation and purification processes. One of the most often application of natural and synthetic zeolites is ammonium removal from natural [15] and wastewaters [16,17].

Ammonia is recognized as one of hazardous water pollutants which is toxic to aquatic organisms and humans [18], hence according to European Legislation, the maximum allowed concentrations (MAC) for ammonia in drinking water is 0.5 mg/L [19]. Zeolites are often used as adsorbents in separation and purification processes and one of the most often application of natural and synthetic zeolites is ammonium removal from natural [15] and wastewaters [20].

Generally, ammonium ion can be coordinated by three ways, specifically through two, three or four oxygen atoms from zeolite crystal [5]. Under conditions of high ammonium coverage, formation of acidic ammonium associations which ensign zeolite NH_4^+ acidity was studied [21]. The comparison of regenerated and native adsorbents adsorption properties in batch and fixed-bed conditions that can prove eventual adsorption power enhancement is accomplished using different methods [22–25]. Accustomed accesses are obtained through the determination of maximal adsorption capacities by utilization of different adsorption isotherm models [26–29], kinetics models of pseudo–first-order and pseudo-second-order [30,31]. Thomas column model was performed for column performance analyze [32–34]. The influence of bed depth, pH, temperature, nature of sorbent and adsorbate as well as the position of breakthrough point (BTP) and surfaces under breakthrough curves were also investigated [35–39]. Breakthrough curves which refer to solid/liquid separation can be derived from the relation of adsorbed adsorbate concentration with time or adsorbate solution effluent volume, respectively [40,41]. Two consequential points can be observed at each breakthrough curve, the BTP and exhaustive point (EP) determining the breakthrough capacity (BTC) and representing exhaustive capacity (EC), respectively. The BTP can be calculated according to the time or volume value corresponding to the relation value of initial (C_{in}) and effluent (C_{out}) adsorbate concentrations expressed as C_{in}/C_{out}, which was defined and reported as 0.5 [42]. It has been shown recently that the BTP value can be examined as a cross-section value of two curves, obtained from graphic relation of C_{out} and $(C_{in} - C_{out})$ vs. time or volume [43]. The EC occurs in the continuous flow system column when adsorbent gets fully saturated and $C_{in} = C_{out}$ [44,45].

The main objective of the present study was to elucidate the possibilities of synthetic zeolite Crystal-Right (CR), previously exhausted by ammonium ions, to remove ammonia from groundwater in dynamic fixed-bed column. After the regeneration procedure by NaCl, NaClO or by their mixtures, the regenerated zeolite was used in eight consecutive tests and ammonia removal was examined. Furthermore, the aim of conducted investigation was the enhancement of CR media adsorption properties by increasing of acid active sites and the determination of the breakthrough, exhaustive and specific adsorption capacities toward groundwater ammonia of purchased and regenerated CR.

Changes of the CR adsorption properties depending of different regeneration modes were proven in this work by a new approach of BTC and EC calculation. In addition, removal efficiency was also used for CR adsorption capabilities determination.

2. Materials and methods

2.1. Water source, zeolite and activated carbon

The groundwater used in this study originated from the Kikinda City waterworks (latitude: 45.8283, longitude 20.4653) in the Vojvodina Province, Northern Serbia. This groundwater is in the use as drinking water and belongs to sodium bicarbonate type (Na^+ ~200 mg/L), the pH value is ~8.2 and the intense yellow color is observed as a result of the dissolved natural organic matter presence (permanganate consumption ~7 mgO_2/L). With respect to groundwater pH, present water contained mostly NH_4^+ form and the composition of present water along with other physicochemical characteristic was previously reported [46].

The ammonia content in this water always exceed 2 mg NH_4^+–N/L and the average value of 2.24 mg NH_4^+–N/L is considerably higher than the MAC for ammonium ion of 0.5 mg/L or 0.39 mg NH_4^+–N/L according to Europe Council recommendations [19].

Synthetic zeolite, type CR-100 (Water Right, Phillipsburg, USA) [47] was used for enhancement of adsorption properties and monitoring of ammonia removal in a dynamic flow

conditions of zeolite fixed-bed column. Sodium aluminosilicate CR-100 is chemically inert, cage-like, tectosilicates in which silicon and aluminum atoms are covalently bonded in tetrahedral arrangements forming pores and channels that permit the non-covalent binding of water and metallic cations. CR-100 is constituted of solid, granular white-light gray crystals with specific gravity at 22°C of 0.686, pore size of approximately 100 Å and specific surface area of 147.16 m^2/g [48]. CR particle size range is presented in Table 1.

Removal of chloramines from CR regeneration wastewater was performed with activated carbon (AC), type Silicarbon K-835 (Silcarbon Aktivkohle GmbH, Kirchhundem, Germany). AC is granulated with density of 500 ± 25 kg/m^3, iodine number 1,050 mg/g and specific surface area of 1,100 m^2/g. AC particle size range was 0.7–1.5 mm.

2.2. Analyses

Investigated groundwater and effluents ammonia concentrations were determined by standard analytical Nessler method using spectrophotometer Hanna C-200 (Hanna instruments, Woonsocket, USA). The method for ammonium nitrogen determination is based upon addition of 1 mL of the potassium sodium tartrate solution into 10 mL of sample improves the color quality and reduces the susceptibility to interferences with calcium and magnesium. Addition of 1 mL of the Nessler reagent into water sample produces a yellow color that is dependent on the NH_4^+–N concentration. By monitoring the color intensity, the concentration of NH_4^+–N was determined by absorbance measurement at the wavelength of 425 nm, directly displayed as mg/L of NH_4^+–N. Spectrophotometer zero point was adjusted with blank unreacted sample. Hanna C-200 instrument measurement range was 0.00 to 10.00 mg/L, resolution 0.01 mg/L, ±0.05 mg/L and ±5% of reading. The Nessler reagent was prepared by dissolution of 70.00 g KI, 100.00 g HgI_2 and 160 g of NaOH in 1,000 mL of deionized water and packed under code HI-93715B-0. Potassium sodium tartrate solution (0.15 mol/L) was prepared by dissolution of 350 g of KNa tartrate into 1,000 mL of deionized water and coded as HI-93715A-0. The instrument directly displays concentrations in mg/L of ammonia nitrogen and thus all the experimentally measured values of inlet water and effluents were presented in mg NH_4^+–N/L. All presented results of groundwater and effluents were the mean values of three repetitions.

2.3. Pilot plant adsorption experiments, regeneration and wastewater treatment

Dynamic fixed-bed experiments were performed in a composite column (structural composite pressure vessel Q-0844 with top opening) and its volume was 38 L. Column also contained a central tube with down distributor of 200 μm fineness as well as a manually controlled four position valve (model 2750, Fleck Ltd., Milwaukee, USA) with up distributor of 200 μm fineness. During the investigations, the control valve enabled four operations which include service flow rate, backwash, brine/slow rinse and fast rinse as well. Backwash of purchased CR is the best way for removal of air from the system, bedding in the media and flushing the system through.

The experimental column was filled with 13,771 g of dry weight CR originated from producer's package. Continuous flow rate meter and total effluent quantity meter were installed at the effluent outlet pipe line. Schematic presentation of the experimental apparatus is shown in Fig. 1. The waterworks water was distributed through suspended solids particle protective 5 μm polypropylene filter cartridge and then fed into the pilot plant downstream. Effluent samples were regularly collected and analyzed for ammonia concentration. Total passed effluent volume and water flow were recorded during the experiment. All dynamic sorption experiments were carried out at 20°C ± 1°C. Adsorption process was stopped when effluent ammonia concentrations were approximately equal to the influent ammonia concentration (in the period of the CR exhaustion). Experimental operating data of the pilot plant are shown in Table 1.

CR regeneration process was performed using NaCl and NaClO, separately or using their mixtures. In the cases when NaCl was used as regenerant, the regeneration process was established in simple ion-exchange mechanism

Table 1
Fixed-bed column operating conditions

Water pressure (bar)	3.0 ± 0.2
Water flow (L/h)	300 ± 10
Water flow rate (m/h)	8.82 ± 0.3
Diameter/length of column (mm)	203/1,118
Internal column cross-section surface (m^2)	0.034
Zeolite particle size range (mm)	0.3–2.4

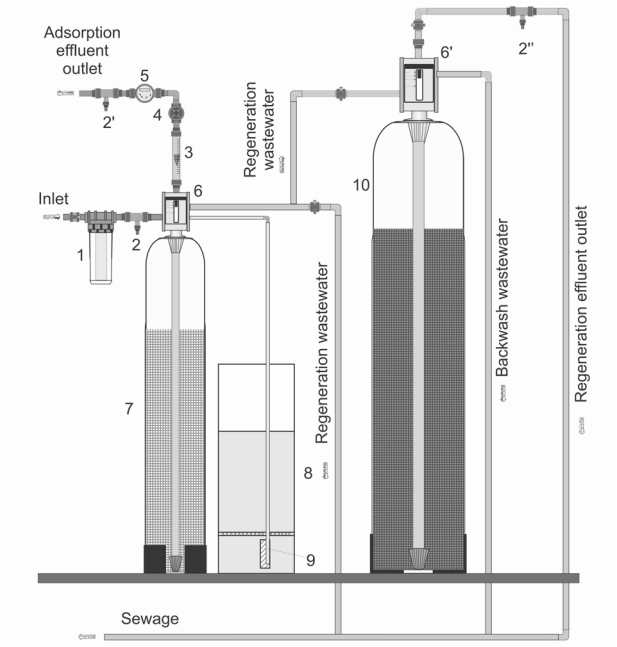

Fig. 1. Schematic description of zeolite fixed-bed pilot plant: 1 – Protective micro filter of 5 μm; 2 – Inlet water sampling tap; 2′ – Effluent water sampling tap; 2′′ – Regeneration effluent sampling tap; 3 – Flow meter; 4 – Adjustable valve; 5 – Water meter; 6 – CR fixed bed control valve; 6′ – AC absorber control valve; 7 – CR packed column; 8 – Brine tank; 9 – Pick up tube with air check; 10 – AC packed column.

and ammonium ions were exchanged with equivalent amounts of sodium ions. Differently from NaCl, the action of NaClO toward ammonia was oxidation to different products mostly represented by chloramines, most frequently by monochloramines [49–51].

Investigated groundwater ammonia adsorption processes (AP) and corresponding ammonia adsorption curves on the original CR (O) and the resulting CR regenerated consecutively for eight times by different chemicals and/or chemical mixtures were examined. In detail, experiments started with adsorption on the original CR (AP A). Adsorption process A was conducted until CR was exhausted. CR was then regenerated using regeneration mode (RGM) A. Every following experiment was conducted using the CR from previous experiment after the regeneration by chemicals listed in Table 2. Regeneration mode expressed via R (A–H) presents CR regeneration with regard to the AP. For example, in the regeneration mode R (A) saturated CR obtained after the adsorption process A was used. In every subsequent RGMs, R (B–H), CR obtained from previous test was regenerated and then used for next adsorption trial. The list of used chemicals, their mixtures, amounts of each regenerant (R_A), specific regenerant loads (R_C) and specific regenerants mixture loads (R_{CT}) are presented in Table 2. The operation steps conducted during regeneration of exhausted CR with each regenerant separately and their mixtures are described in Table 3. In the cases of regeneration with NaCl and NaClO as single regenerant (RGMs R (A–C)), steps 2, 3 and 5, respectively were not performed.

Chloramines originated by CR media regeneration are disinfectants of low molecular weight in form of neutral vapor. They posse characteristic intense smelt and need to be eliminated or neutralized in CR media regeneration wastewater before its discharge in sewage installation. There are some methods for chloramines neutralizing of which the AC adsorption is most effective one [50]. In the processes in which NaClO was used as the regenerant, either alone or in the mixture with NaCl, the regeneration effluent was treated on the AC absorber for neutralization of chloramines prior to its discharge. Packed AC column for chloramines removal was performed in a composite column (structural composite pressure vessel Q-1354). Volume of the vessel with top opening was 103 L. Column also contained a central tube with down distributor of 200 μm fineness as well as a manually controlled four position valve (model 2850, made by company Fleck), with up distributor of 200 μm fineness. During the process control valve enabled three operations: service flow rate, backwash and fast rinse, as well. Physicochemical and other processes that could appear in contact of the AC with the regeneration effluent were not the scope of this investigation, and the absence of specific chloramines smelt in wastewater and surrounding air were satisfactory indicator of successful absorber function.

Table 2
Survey of adsorption experiments with original and regenerated CR

AP	RGM	Chemical	R_A (mol)	R_C (mmol/g)	R_{CT} (mmol/g)
A	O	–	–	–	
B	R (A)	NaCl	136.75	9.93	9.93
C	R (B)	NaClO	6.44	0.47	0.47
D	R (C)	NaClO	12.88	0.94	0.94
E	R (D)	NaCl	136.75	9.93	10.09
		NaClO	2.15	0.16	
F	R (E)	NaCl	136.75	9.93	10.40
		NaClO	6.44	0.47	
G	R (F)	NaCl	136.75	9.93	10.87
		NaClO	12.88	0.94	
H	R (G)	NaCl	136.75	9.93	11.33
		NaClO	19.33	1.40	
I	R (H)	NaCl	273.5	19.86	20.80
		NaClO	12.88	0.94	

Note: AP, adsorption process; RGM, regeneration mode; R_A, amount of regenerant; R_C, specific regenerant load; R_{CT}, specific regenerants mixture load.

2.4. Determination of CR column ammonia adsorption characteristics

Changes of groundwater ammonia adsorption presented by measured effluent ammonia concentrations during the experiments are shown in the dependence to cumulative time (Στ) and number of effluent's bed volumes (BV), as well. In general, the overview of adsorption process kinetics toward to the start, breakpoint and final equilibrium stages can be presented by shapes of these curves. The determination of ammonia adsorption characteristics during zeolite fixed-bed experiments usually include calculation of several parameters such as bed volume and different ammonia amounts, which enclose the overall amount that entered in the column, the amount that came into contact with the CR, the effluent amount and the CR sorbed amount. Total volume of water that passed through the CR bed was expressed as BV. This parameter is a dimensionless quantity which expresses the water volume as a multiple of the resin bed volume [52]

$$\mathrm{BV} = V_{\mathrm{out}}/V_{\mathrm{CR}} \tag{1}$$

where V_{out} (L) is the cumulative volume of effluent passing through at the time of sampling; V_{CR} (L) is the CR volume which amounted 28 L in all experiments.

Table 3
The CR regeneration procedure

Operation step	Operation	Duration time (min)
1	Backwash	10
2	NaCl sucking	5
3	NaClO sucking	5
4	Pause	20
5	NaCl sucking + slow rinse	55
6	Fast rinse	15

Overall ammonia amount in the total volume of groundwater that entered in the column during the experiment, Q_{total} (mg NH_4^+–N) was calculated as follows:

$$Q_{total} = V_{total} \times C_{in} \quad (2)$$

where V_{total} (L) is the total volume of the water treated in the experiment; C_{in} (mg NH_4^+–N/L) is the influent ammonia concentration.

The ammonia amount that came into contact with the CR, Q_{in} (mg NH_4^+–N) was based on the measured volume of groundwater between two sampling points that passed through the bed in real experimental time and was calculated as follows:

$$Q_{in} = V_{out} \times C_{in} \quad (3)$$

The effluent ammonia amount at the each sampling point was calculated using Eq. (4)

$$Q_{out} = V_{out} \times C_{out} \quad (4)$$

where Q_{out} (mg NH_4^+–N) is the ammonia amount determined in the effluent.

The ammonia amount after collecting the effluent volume in the regard to an instantaneous sample, represented the adsorbed ammonia amount onto the CR, was calculated as follows:

$$Q_{ads} = Q_{in} - Q_{out} \quad (5)$$

where Q_{ads} (mg NH_4^+–N) is the adsorbed ammonia amount.

The Q_{ads} is a very important parameter for the estimation of adsorbent quality toward adsorbate under known and controlled conditions, as well as about different regeneration chemicals efficiency. For quantitative presentation of the column capacity, values of Q_{ads}, Q_{in} and Q_{out} were used and ratios of Q_{ads}/Q_{in} and Q_{out}/Q_{in}, both vs. BV, $\Sigma\tau$ and V_{out} enabled simultaneous overview of adsorbed and passed ammonia in fixed-bed column, respectively. The relative breakthrough capacity (BTCX) and exhausting capacity (ECX) values were calculated from the equations Q_{ads}/Q_{in} vs. BV, $\Sigma\tau$ and V_{out}, as explained in Eqs. (6) and (7), respectively

$$\mathrm{BTCX} = \int_{X_{min}}^{X_{BTP}} (\alpha \times X^2 + \beta \times X + \gamma) \times dX \quad (6)$$

$$\mathrm{ECX} = \int_{X_{min}}^{X_{max}} (\alpha \times X^2 + \beta \times X + \gamma) \times dX \quad (7)$$

where X represents the BV, $\Sigma\tau$ or V_{out} and α, β and γ are empirically obtained quadratic equation coefficients.

The BTC and EC values for different X-axis units were calculated as definite integrals exactly as the limit and summation of minimum and corresponding values of the BTP and extreme values, respectively. The obtained data were found as the net areas between a function and the X-axis. The BTCX and ECX surfaces are dimensionless relative values of the BTC and EC, useful for comparisons between different adsorption conditions or applied adsorbent regeneration procedure effects, in regard to the same chosen X-axis physical unit only.

Values of the BTCX and ECX were normalized to obtain the specific adsorption power coefficients (APC), the APC breakthrough point (APC_{BTP}) and APC exhausting point (APC_{EP}) as shown in Eqs. (8) and (9)

$$\mathrm{APC_{BTP}} = \mathrm{BTCX/BTP(X)} \quad (8)$$

$$\mathrm{APC_{EP}} = \mathrm{ECX/EP(X)} \quad (9)$$

where the BTP(X) and EP(X) are values of the BTP and EP in the dependence of physical unit shown at X-axis, respectively.

The values of the APC_{BTP} and APC_{EP} can be comparable in different adsorption processes regardless of physical unit used for the calculation. Both, the APC_{BTP} and APC_{EP} are dimensionless and their numerical values could be in the range between 0 and 1. The higher the values of the APC_{BTP} and APC_{EP} signify more powerful adsorbent for the chosen sorbate. Also, adsorption power is higher if the $APC_{BTP} > APC_{EP}$. In general, if affinity of the adsorbent to the sorbate is low and the adsorption process is weak, the intersection of breakthrough curves obtained from graphical relation of the ratios of Q_{ads}/Q_{in} and Q_{out}/Q_{in}, both vs. BV, $\Sigma\tau$ and V_{out}, respectively, does not appear and the determination of the BTP is disabled.

According to previous calculations, obtained values of the APC_{BTP} and APC_{EP} depend on the data used in Eqs. (6)–(9). If the obtained APC_{BTP} and APC_{EP} values in the relation to the BV, $\Sigma\tau$ and V_{out} were similar, respectively, the further application of mentioned equations could include only the BV, as previously reported [42,43].

Exact values of both, the breakthrough and exhausting column capacities, CC_{BTP} and CC_{EP} (mg NH_4^+–N), respectively, were calculated using Eqs. (10) and (11)

$$\mathrm{CC_{BTP}} = \sum_{i=1}^{i=\mathrm{BTP}} Q_{ads}(\mathrm{BTP}) \quad (10)$$

$$\mathrm{CC_{EP}} = \sum_{i=1}^{i=n} Q_{ads}(n) \quad (11)$$

where variable n is the number of sampling points during the fixed-bed investigation; the Q_{ads} value for $i = n$ is equal to the Q_{ads} value for the EP.

Fixed-bed data values of the CC_{BTP} and CC_{EP} and their relations are experimental results comparable with the calculated APCs data obtained by the virtue of modeling.

Removal efficiency that was used to present enhancements of synthetic zeolite active sites was calculated using Eq. (12).

$$\eta = 1 - \frac{C_{out}}{C_{in}} \times 100 \quad (12)$$

3. Results and discussion

During CR fixed-bed experiments changes of effluent ammonia concentration in time throughout the course of the experiment represented an essential overview of the adsorption process kinetics. The graphical description of all experimental points that presented these dependences was shown in Fig. 2. As can be seen a very similar experimental point layout, and shapes of regression curves, representing the BV influence on concentration changes were also obtained. Presented experimental data (Figs. 2(a) and (b)) indicated that the overall process can be described with three separate parts. The first part was characterized by great ammonia adsorption, while second part showed sharp increase of effluent concentrations and third one was specific to influent ammonia value convergence. The duration of these three steps of adsorption processes were previously elucidated in similar study and obtained values were in congruence with reported results [43]. The dissipations of experimental points with regard to presented regression curves belonging to the AP A can be observed (Fig. 2). The lowest ammonia adsorption and highest dissipation of experimental points from regression curve A was registered in the case of the RGM R (A) during the AP B.

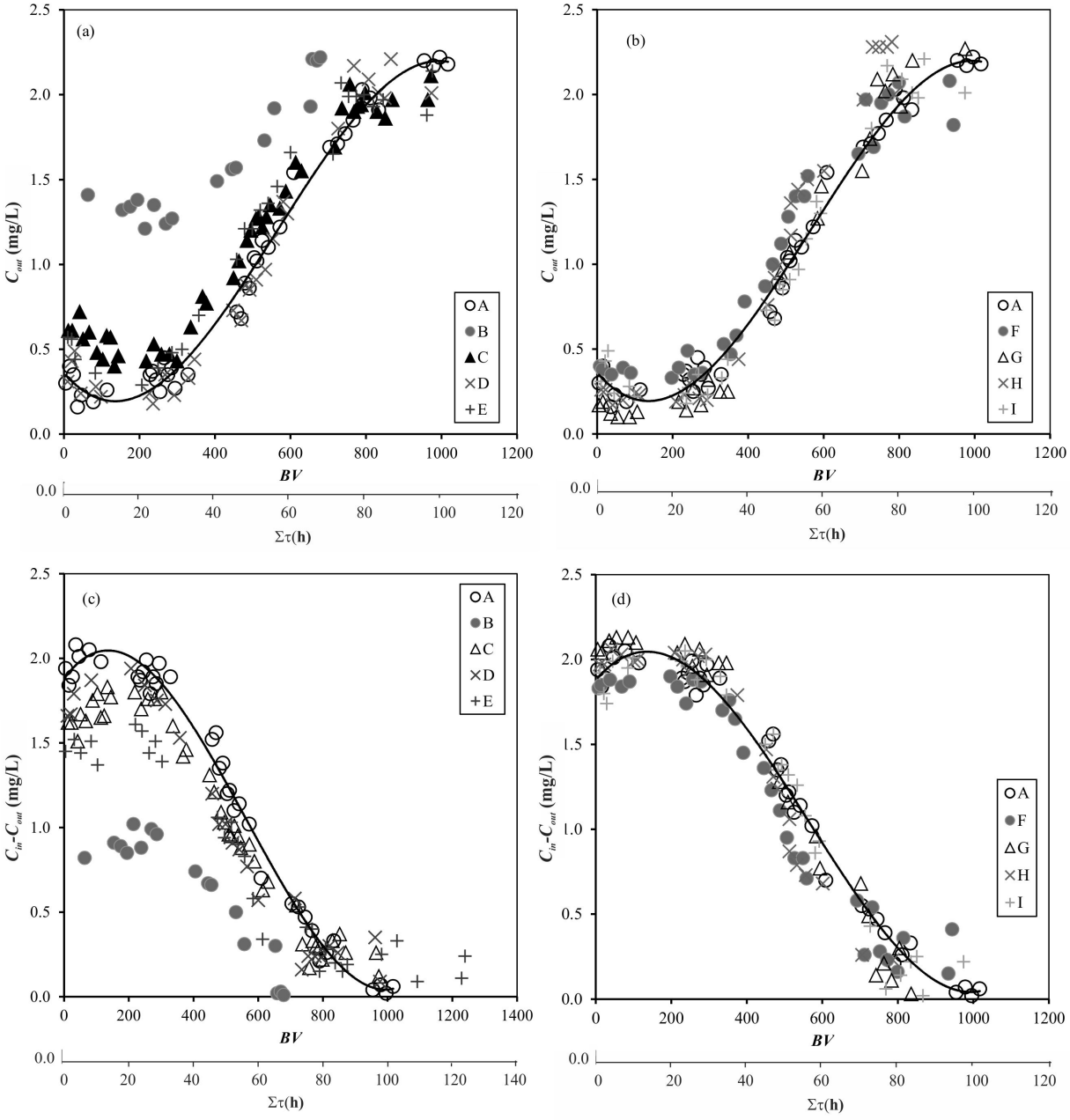

Fig. 2. Comparison of ammonia effluent concentration changes during time and the *BV* during the AP A–E (a) and during the AP A and AP F–I (b). Changes of adsorbed ammonia concentration values in dependence to the Στ and *BV* during the AP A–E (c) and during the AP A and AP F–I (d). The depicted curves present polynomial regressions of AP A experimental points.

Regeneration processes conducted by RGMs R (A–C) were performed with the use of individual low regenerants quantities (Table 2) and obtained results (experimental points B–D), respectively, showed inadequate results on the CR occupied active sites discharging in comparison with the CR (O) (Fig. 2(a)). Significantly better adsorbed ammonia removal was gained by the mixture of regenerants (combined action of NaCl and NaClO) and a very big accordance of experimental points (F–I) can be seen especially with regard to the curve A (Fig. 2(b)). Characteristic decreasing trend of the curve A and experimental points shown in Figs. 2(c) and (d), assigning mirror symmetry toward corresponding curve presented in Figs. 2(a) and (b).

During all experiments, values of the Q_{in}, Q_{out} and Q_{ads} were calculated for the each sampling point using Eqs. (3)–(5), respectively. The BTP and EP values were determined from the plots Q_{ads}/Q_{in} vs. BV and Q_{out}/Q_{in} vs. BV, respectively, and represented the breakthrough curves, as previously mentioned and shown in Fig. 3. These curves enabled access to observation of dynamical changes of Q_{out} increase and Q_{ads} decrease. In general, obtained experimental points of stated relations could be the best fitted to a polynomial regression of the second order, in mathematical sense. Cross-points of Q_{ads}/Q_{in} and Q_{out}/Q_{in} vs. BV, Στ and V_{out} curves, respectively, were exactly at value of 0.5 at *Y*-axis in all three cases, so, all these relations promote to breakthrough curves. This means that the BTP can be simply determined as corresponding *X*-axis value for physical units of BV, Στ and V_{out}. The BTP values were calculated as an intersection of these curves corresponding pairs. The only exception was in the case of adsorption procedure B, where it was not possible to define the BTP, as shown in Fig. 3(b), and therefore the BTC value could not be calculated. The BTP value for original CP was 572.79 BV, but in adsorption procedure H and I, according to obtained results, just somewhat lower values of 512.89 and 554.32 BV, respectively, were obtained, indicating that efficient ammonia removal could be achieved using adequately regenerated CR (Table 4). Exhausting points were determined as a

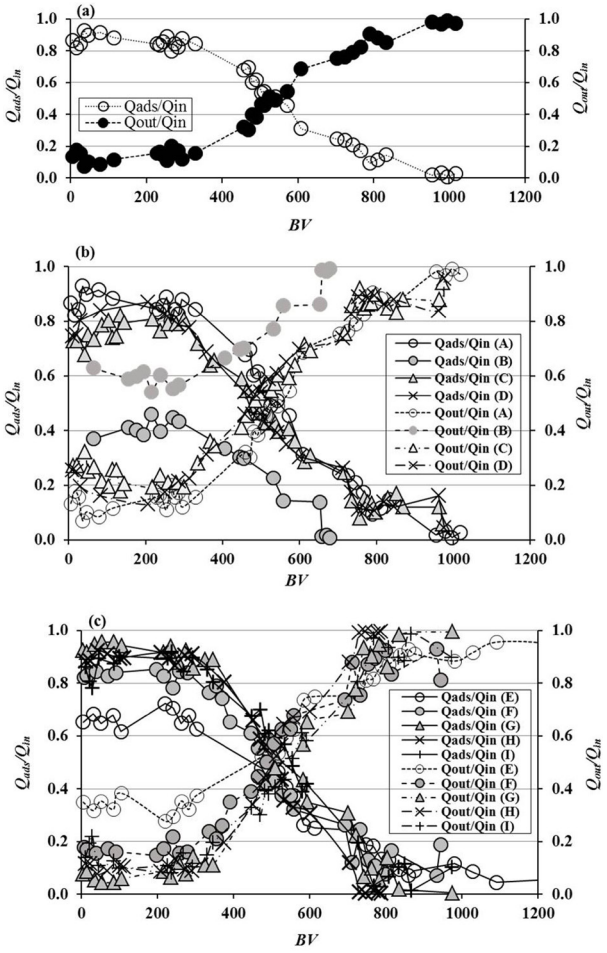

Fig. 3. Breakthrough curves of ammonia adsorption: on original CR obtained during AP A (a) and on differently regenerated CRs used in adsorption processes B–E (b) and used in adsorption processes F–I (c).

Table 4
The original and regenerated CR fixed-bed column adsorption characteristics

AP	A	B	C	D	E	F	G	H	I
Q_{total} ($mgNH_4^+$–N)	63,793	42,598	61,009	61,219	77,706	59,221	61,141	49,347	61,094
R^2	0.9463	0.9593	0.9205	0.9048	0.9008	0.9029	0.9481	0.9726	0.9217
BTP (BV)	572.79	–	485.18	478.93	473.96	487.82	509.07	512.89	554.32
BTC	402.51	–	322.36	318.27	270.71	355.01	413.26	387.06	419.18
APC_{BTP}	0.74	–	0.66	0.66	0.57	0.73	0.81	0.75	0.76
CC_{BTP} (mg)	26,292	–	21,709	22,242	18,144	23,354	25,717	25,317	27,217
EP (BV)	1,017.11	679.18	972.71	976.07	1,238.93	944.21	974.82	786.79	974.07
EC	488.52	181.91	446.01	417.80	395.36	482.42	502.88	423.05	519.08
APC_{EP}	0.48	0.27	0.46	0.43	0.32	0.51	0.52	0.54	0.53
CC_{EP} (mg)	30,779	12,935	28,549	29,213	25,850	28,964	30,871	28,241	31,056
BTC/EC	0.82	–	0.72	0.76	0.68	0.73	0.82	0.91	0.81

Note: AP, adsorption process; Q_{total}, overall ammonia amount in the total volume of groundwater that entered in the column during the experiment; R^2, regression coefficients of breakthrough curves Q_{ads}/Q_{in} vs. BV; BTP, breakthrough point; BTC, breakthrough capacity; APC_{BTP}, specific adsorption power coefficients breakthrough point; CC_{BTP}, breakthrough column capacities; EP, exhaustive point; EC, exhaustive capacity; APC_{EP}, specific adsorption power coefficients exhaustive point; CC_{EP}, exhaustive column capacity.

Q_{ads}/Q_{in}, that is, Q_{out}/Q_{in} points corresponding to the largest BV value. At the basis of determined BTP and EP, the BTCX and ECX values were calculated using Eqs. (6) and (7), and then normalized toward BV according to Eqs. (8) and (9). The obtained results of column adsorption parameters are presented in Table 4. According to calculations based on the applied independent variables (BV, Στ and V_{out}), the obtained APC_{BTP} and APC_{EP} values had a standard deviation of 0.0118. Therefore, as mentioned previously further calculations included only BV (Eqs. (10) and (11)) [42,43].

The position of experimental points in Figs. 3(b) and (c), for each experiment, in comparison with adsorption procedure A (Fig. 3(a)) indicated congruence with Q_{ads} of the CR (O). More or less similarity of post-regeneration adsorption processes to the adsorption process on the original CR (Figs. 3(a)–(c)) confirmed preliminary hypothesis of different regeneration modes effect, defined by concentration plots (Fig. 2). More distinct CR restoration column capacity was recognized in RGMs R (E–H) as shown in Fig. 3(c), due to the facts that the quotients of Q_{ads}/Q_{in}, and Q_{out}/Q_{in}, with regard to the highest BV values of each experiment, were found to amount very near to 0 and 1, respectively, and were similar to values shown in Fig. 3(a). The curves of RGMs R (A–D) depicted in Fig. 3(b), did not show stated values, except for process R (A). Just this example, which demonstrated the shorter duration of column adsorption process, denoted that the regeneration process could be partially successful but improper. The Na^+ and NH_4^+ were successfully replaced by ion-exchange creating deficient number of active sites with regard to the original CR. The higher part of adsorbent pores remained filled, and the AP B achieved saturation already at ~700 BV. More properly defined RGMs showed power of selected regenerants emptying adsorbent pores and creating new active sites. Decreased regeneration results were in both cases observed with pure NaCl and NaClO solutions separately (AP B–D). Obviously, selected NaCl/NaClO molar ratio applied in R (H) ensured parallel ion-exchange and oxidation paths which associated mechanisms brought to excellent regeneration results. Nevertheless, all obtained BTPs values for regenerated CR were lower from ~3% to ~21% than those found in the original CR.

The exhausting point values depended of the duration of each sorption process, until appearance of C_{out}–C_{in}. The volume of treated water did not influence ECs values, thus, representativeness and types of CR active sites probably had the leading influence. The interrelationship of corresponding BTCs and ECs of ~68% to ~91% indicated that more positions of CR active sites were filled, and that the dominant part of sorption processes was finished until the BTPs appear. Also, as the ratio of BTC/EC was higher, the CC_{BTP} and CC_{EP} values were higher as well. The results of calculated column capacities and APC corresponding to BTP and EP values are shown in Fig. 4.

The APC_{BTP} and APC_{EP} for some adsorption processes showed better results in comparison to observed APCs for the original CR (Table 4). The reason for this was probably that high quantities of both regenerants in beneficial ratios brought in significant adsorption active sites enhancement. Particularly APs G, H and I achieved the highest APC_{BTP} of 0.81, 0.75 and 0.76 and APC_{EP} of 0.52, 0.54 and 0.53, respectively. These observations indicated stronger bonding of ammonia to those CR than the original CR and other regenerated CRs (Table 4). The distinct RGM was R (F) with the highest APC in BTP of 0.81 and observed results indicated that this adsorption process showed the highest ammonia adsorption.

Unsatisfactory regeneration effects were expressed particularly on the RGMs R (B–E) (Fig. 3(b)). The exception was only R (A) applied in the AP B, where the lowest adsorption properties were a consequence of deficiently but properly derived CR regeneration. Obviously, the most of ammonia was bonded to CR crystalline structure by electrostatic adsorption and was successfully removed in strong oxidation process by NaClO in engaged regeneration modes R (F–H) (Fig. 3(c)).

The overall CC_{EP} and total amount of regenerants (R_{AT}), both expressed in moles for each RGM showed the huge regenerants quantity to which adsorbed NH_4^+ were exposed during the all applied regeneration processes. This is clearly visible from the molar ratio values of R_{AT}/CC_{EP} showed in Table 5. Obtained molar ratios demonstrated that in all investigated CR regeneration modes, regenerants were not added in stoichiometrically equivalent quantity, but in high excess as already reported by Deng [53]. The multiple quantity of NaCl obviously was not sufficient to exchange NH_4^+

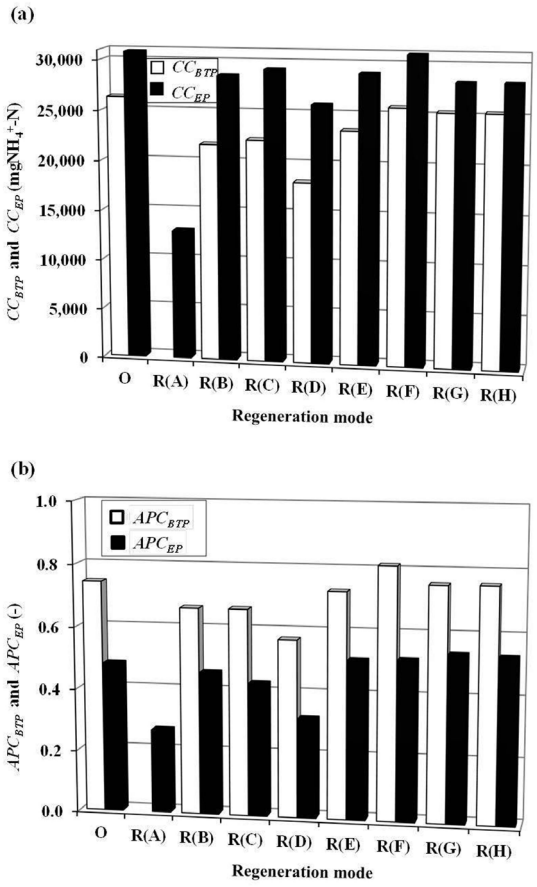

Fig. 4. Survey of established adsorption properties corresponding to the calculated breakthrough and exhausting points of different ammonia adsorption processes on the original and regenerated synthetic zeolite CR: column capacities (a) and adsorption power coefficients (b).

and Na^+ in RGM R (A). Interactions between NaClO alone and exhausted CR during RGMs R (B and C) also resulted in unsatisfactory regeneration. Only different combinations of NaCl and NaClO successfully regenerated exhausted CR and enhanced its adsorption properties. The best results of CR adsorption properties enhancement were obtained in the RGMs R (F–H), which were conducted using mixture of NaCl and NaClO in molar ratios of 10.62:1, 7.07:1 and 21.24:1, respectively. These facts are a consequence of NaCl and NaClO conjunct activities toward activation of divalent and trivalent CR media sites. Ammonia ions affects only monovalent active sites of the original CR and only NaCl regenerated CR as well, which contain Na^+ exchangeable ions [1]. In the presence of NaClO, hydrogen ions as a product of hydrolysis process took place at polyvalent CR sites. The Na^+ from NaCl can also displace hydrogen ions by increasing the available surface for ammonia adsorption in the next adsorption experiment. Hence, the axiom that Na^+ from NaClO did not significantly affected the exhausted CR regeneration or adsorption properties enhancement was proven during R (B) and R (C). Effects of NaCl sodium ions exchange with ammonia ions were expressed only in experiments, where NaClO was in sufficient excess to provide new polyvalent active sites consisting of hydrogen ions. The obtained results confirmed previous investigations of aluminosilicate zeolites acid sites nature [54,55]. Hence, as a consequence of substitution product of neutral charged silicon atoms in tetrahedral positions with aluminum atoms "–1" charge occurred. Originated negative framework charges were balanced by hydroxyl protons or extra framework metal cations forming strong Brønsted acid sites and weak Lewis acid sites, respectively. These formed active sites were responsible for catalytic activity of the CR media which was approved by enhanced specific adsorption capacity. In the same time, other parallel chemical reactions took place. It is supposed that atomic oxygen oxidized some amount of adsorbed dissolved organics traces, and obtained gaseous chlorine created chloramines in reaction with ammonia. All these physicochemical processes and chemical reactions contributed to amplification of the CR media possibilities for ammonia adsorption.

Influence of cumulative time on removal efficiency for all adsorption processes is given in Fig. 5. As can be seen in Fig. 5(a) native CR had the highest removal efficiency at the start of adsorption process for approximately 32 h, where η was in the range of 85%–95%. AP B showed the lowest removal efficiency which was also confirmed with the lowest APC_{EP} and CC_{EP} values presented in Table 4. AP C–E had lower values of η than original CR almost throughout all experimental time with the exception at the end of adsorption process. Considering low values of removal efficiency at this point of approximately 10%–20% it can be concluded that no significant changes were made on zeolite active sites. Obtained data for AP G, H and I (Fig. 5(b)) proved that usage of optimal regeneration chemicals mixture can be used for enhancement of zeolite active sites, especially in the zone of zeolites largest adsorptive power, at the beginning of adsorption process until ~40 h, with regard to original zeolite. When C_{in} value is taken into consideration, removal efficiency needs to be <85.60% in order to achieve MAC of 0.39 NH_4^+–N/L. This value is achieved precisely in above stated time range in AP G, H and I.

Table 5
The molar ratio of total regenerants and adsorbed ammonia amounts

RGM	R_{AT} (mol)	R_{AT}/CC_{EP}
R (A)	136.75	231.19
R (B)	6.44	32.85
R (C)	12.88	28.44
R (D)	138.90	287.80
R (E)	143.19	280.06
R (F)	149.63	312.85
R (G)	156.08	261.31
R (H)	286.38	191.84

Note: RGM, regeneration mode; R_{AT}, total amount of regenerants; CC_{EP}, exhaustive column capacity.

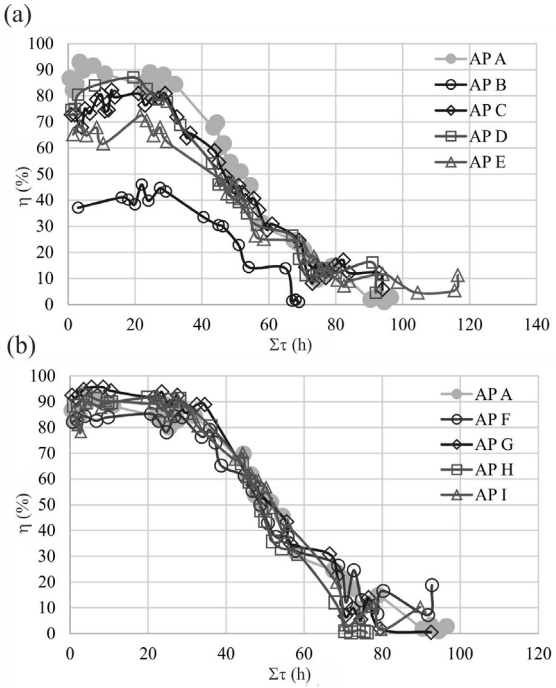

Fig. 5. Effect of overall process duration on adsorption processes removal efficiency (a) AP A-E; (b) AP A, F-I.

4. Conclusions

The novelty of presented work was the enhancement of adsorption characteristics in regenerated synthetic zeolites by creation of both NH_4^+ and H^+ active sites, and the new approach to the adsorbed ammonia amount calculation. Obtained breakthrough points, enabled determination of the capacity values which were normalized to the BV and specific APC were established. The emphasis of present work was on the creation of new proton active sites due to the oxidation power of NaClO in conjunction with ion-exchange caused by NaCl, which were partially contributed to active sites moiety together with Na^+ ions. Furthermore, the use of natural groundwater enabled the occupation of zeolite active sites by NH_4^+ and other ions. Therefore, the obtained enhancement of adsorption characteristics in regenerated synthetic zeolites enables effective ammonia removal.

Investigated ion-exchange and adsorption processes of ammonium ions onto different CR media showed significant influence of NaClO high molar excess on adsorption properties enhancement. Different breakthrough and exhaustive point values associated with particular CR regeneration modes presented significant demonstration of wide zeolite possibilities to create newly differently constituted specific active sites with regard to native CR. During the regeneration processes, Na^+ originated from NaCl were exchanged with bonded NH_4^+ and hydrogen ions originated from Na-hypochlorite hydrolyses were exchanged with NH_4^+ to previously bonded ammonium monovalent sites and occupied other polyvalent CR active sites enabling adsorption area ready for NH_4^+ in the next adsorption cycle. During Na-hypochlorite presence in the regeneration solution new redistribution of active sites was observed. During CR regeneration active sites which bonded ammonium ion were exchanged with both Na^+ and H^+ cations, different at every NaCl–Na-hypochlorite ratio. Total sites number is approximately constant and only ratio between Na^+ and H^+ was changed. The BTP values dependence of different RGMs was established as a mathematical approach for calculations of the CC_{BTP} as a dominant part of each investigated adsorption process. Due to described phenomena of protons bonding to zeolite's oxygen bridges, BPCs and ECs of investigated synthetic zeolite fixed-bed column capacity toward NH_4^+ was enhanced with regard to the original CR. Established APCs in BTP and EP as a simple way for the comparison of column capacity magnitude with regard to the RGMs were in good congruence with experimentally obtained data for total adsorbed ammonia. Better ammonia bonding onto regenerated CRs was observed during adsorption processes G, H and I than the original CR and other regenerated CRs. This was evidenced by the highest APC_{BTP} of 0.81, 0.75 and 0.76 and APC_{EP} of 0.52, 0.54 and 0.53, in AP G, H and I, respectively. Larger part of ammonia was bonded to CR crystalline structure by electrostatic adsorption and was successfully eliminated in strong oxidation process by NaClO in engaged regeneration modes R (F–H). The best results of CR adsorption properties enhancement were obtained in the RGMs R (F–H), which were conducted using mixture of NaCl and NaClO in molar ratios of 10.62:1, 7.07:1 and 21.24:1, respectively. These facts are a consequence of NaCl and NaClO conjunct activities toward activation of divalent and trivalent CR media sites. In addition, adsorption processes G, H and I presented better removal efficiency than other adsorption processes. Ammonia removal efficiency was higher in three adsorption processes that were conducted with regenerated zeolite than removal efficiency obtained with native non-regenerated zeolite. The obtained results showed that the right selection of regenerants and regeneration conditions enabled the significant enhancement of synthetic zeolite adsorption properties, as well as their possible applications.

References

[1] G.M. Zhidomirov, A.A. Shubin, A.V. Larin, S.E. Malykhin, A.A. Rybakov, In: J. Leszczynski, M.K. Shukla, Molecular Models of the Stabilization of Bivalent Metal Cations in Zeolite Catalysts, Practical Aspects of Computational Chemistry I, Springer, Netherlands, 2012, pp. 579–643.

[2] R.M.A. Roque-Malherbe, The Physical Chemistry of Materials: Energy and Environmental Applications, CRC Press, Boca Raton, 2009.

[3] N. Danilina, F. Krumeich, S.A. Castelanelli, J.A. van Bokhoven, Where are the active sites in zeolites? Origin of aluminum zoning in ZSM-5, J. Phys. Chem. C, 114 (2010) 6640–6645.

[4] H.E. van der Bij, B.M. Weckhuysen, Phosphorus promotion and poisoning in zeolite-based materials: synthesis, characterisation and catalysis, Chem. Soc. Rev., 44 (2015) 7406–7428.

[5] S. Li, F. Deng, In: F.-S. Xiao, X. Meng, Solid-State NMR Studies of Zeolites, Zeolites in Sustainable Chemistry: Synthesis, Characterization and Catalytic Applications, Springer Berlin Heidelberg, Berlin, Heidelberg, 2016, pp. 231–268.

[6] D. Barthomeuf, In: B. Imelik, C. Naccache, Y. Ben Taarit, J.C. Vedrine, G. Coudurier, H. Praliaud, Structural and Physicochemical Aspects of Acidic Catalysis in Zeolites, Studies in Surface Science and Catalysis, Elsevier, Amsterdam, 1980, pp. 55–64.

[7] E.G. Derouane, J.C. Védrine, R.R. Pinto, P.M. Borges, L. Costa, M.A.N.D.A. Lemos, F. Lemos, F.R. Ribeiro, The acidity of zeolites: concepts, measurements and relation to catalysis: a review on experimental and theoretical methods for the study of zeolite acidity, Cat. Rev., 55 (2013) 454–515.

[8] A.S.M. Junaid, M.M. Rahman, G. Rocha, W. Wang, T. Kuznicki, W.C. McCaffrey, S.M. Kuznicki, On the role of water in natural-zeolite-catalyzed cracking of athabasca oilsands bitumen, Energy Fuels, 28 (2014) 3367–3376.

[9] M. Šiljeg, L. Foglar, M. Kukučka, The ground water ammonium sorption onto Croatian and Serbian clinoptilolite, J. Hazard. Mater., 178 (2010) 572–577.

[10] R. Leyva-Ramos, G. Aguilar-Armenta, L.V. Gonzalez-Gutierrez, R.M. Guerrero-Coronado, J. Mendoza-Barron, Ammonia exchange on clinoptilolite from mineral deposits located in Mexico, J. Chem. Technol. Biotechnol., 79 (2004) 651–657.

[11] E. Fosso-Kankeu, A.-F. Mulaba-Bafubiandi, J.T. Modipe, E.S. Maroga, Regeneration and Reuse of Clinoptilolite for Recovery of Copper and Cobalt from Aqueous Solutions, International Conference on Mining, Mineral Processing and Metallurgical Engineering, 2013.

[12] Y. Nakasaka, T. Tago, H. Konno, A. Okabe, T. Masuda, Kinetic study for burning regeneration of coked MFI-type zeolite and numerical modeling for regeneration process in a fixed-bed reactor, Chem. Eng. J., 207–208 (2012) 368–376.

[13] Z. Danková, I. Štyriaková, A. Mockovčiaková, I. Štyriak, M. Orolínová, Bioleaching as possible method of sorbent regeneration, Bioeng. Biosci., 1 (2013) 31–36.

[14] G. Gruett, Contaminant Removal Made Easy, Water Quality Products, 2007.

[15] E. Chmielewská, Ammonia removal using the bed filtration across the abundantly available clinoptilolite-rich tuff, Int. J. Environ. Pollut. Solution, 2 (2014) 20–31.

[16] Y.-C. Chung, D.-H. Son, D.-H. Ahn, Nitrogen and organics removal from industrial wastewater using natural zeolite media, Water Sci. Technol., 42 (2000) 127–134.

[17] A.R. Rahmani, A.H. Mahvi, A.R. Mesdaghinia, S. Nasseri, Investigation of ammonia removal from polluted waters by clinoptilolite zeolite, Int. J. Environ. Sci. Technol. (Tehran), 1 (2004) 125–133.

[18] H. Wang, H. Gui, W. Yang, D. Li, W. Tan, M. Yang, C.J. Barrow, Ammonia nitrogen removal from aqueous solution using functionalized zeolite columns, Desal. Wat. Treat., 52 (2014) 753–758.

[19] E.U. Council, Council Directive 98/83 EC on the Quality of Water Intended for Human Consumption, Official Journal of European Communities, 1998.

[20] H. Huang, L. Yang, Q. Xue, J. Liu, L. Hou, L. Ding, Removal of ammonium from swine wastewater by zeolite combined with chlorination for regeneration, J. Environ. Manage., 160 (2015) 333–341.

[21] F. Lónyi, J. Valyon, A TPD and IR study of the surface species formed from ammonia on zeolite H-ZSM-5, H-mordenite and H-beta, Thermochim. Acta, 373 (2001) 53–57.

[22] N. Saman, K. Johari, S.T. Song, H. Mat, Silver adsorption enhancement from aqueous and photographic waste solutions

by mercerized coconut fiber, Sep. Sci. Technol., 50 (2015) 937–946.
[23] A.D. Dwivedi, S.P. Dubey, M. Sillanpää, Y.-N. Kwon, C. Lee, Distinct adsorption enhancement of bi-component metals (cobalt and nickel) by fireweed-derived carbon compared to activated carbon: incorporation of surface group distributions for increased efficiency, Chem. Eng. J., 281 (2015) 713–723.
[24] K. Mukherjee, A. Kedia, K. Jagajjanani Rao, S. Dhir, S. Paria, Adsorption enhancement of methylene blue dye at kaolinite clay-water interface influenced by electrolyte solutions, RSC Adv., 5 (2015) 30654–30659.
[25] G. Zeng, Y. Liu, L. Tang, G. Yang, Y. Pang, Y. Zhang, Y. Zhou, Z. Li, M. Li, M. Lai, X. He, Y. He, Enhancement of Cd(II) adsorption by polyacrylic acid modified magnetic mesoporous carbon, Chem. Eng. J., 259 (2015) 153–160.
[26] A. Qajar, M. Peer, M.R. Andalibi, R. Rajagopalan, H.C. Foley, Enhanced ammonia adsorption on functionalized nanoporous carbons, Microporous Mesoporous Mater., 218 (2015) 15–23.
[27] V.K. Gupta, I. Ali, T.A. Saleh, M.N. Siddiqui, S. Agarwal, Chromium removal from water by activated carbon developed from waste rubber tires, Environ. Sci. Pollut. Res., 20 (2012) 1261–1268.
[28] V.K. Gupta, R. Kumar, A. Nayak, T.A. Saleh, M.A. Barakat, Adsorptive removal of dyes from aqueous solution onto carbon nanotubes: a review, Adv. Colloid Interface Sci., 193–194 (2013) 24–34.
[29] A. Khosravi, M. Esmhosseini, S. Khezri, Removal of ammonium ion from aqueous solutions using natural zeolite: kinetic, equilibrium and thermodynamic studies, Res. Chem. Intermed., 40 (2014) 2905–2917.
[30] A. Alshameri, C. Yan, Y. Al-Ani, A.S. Dawood, A. Ibrahim, C. Zhou, H. Wang, An investigation into the adsorption removal of ammonium by salt activated Chinese (Hulaodu) natural zeolite: kinetics, isotherms, and thermodynamics, J. Taiwan Inst. Chem. Eng., 45 (2014) 554–564.
[31] R. Fu, Y. Yang, Z. Xu, X. Zhang, X. Guo, D. Bi, The removal of chromium (VI) and lead (II) from groundwater using sepiolite-supported nanoscale zero-valent iron (S-NZVI), Chemosphere, 138 (2015) 726–734.
[32] J.T. Nwabanne, P.K. Igbokwe, Adsorption performance of packed bed column for the removal of lead(II) using oil palm fibre, Int. J. Appl. Sci. Technol., 2(2012) 106–115.
[33] Y. Yan, X. Sun, F. Ma, J. Li, J. Shen, W. Han, X. Liu, L. Wang, Removal of phosphate from etching wastewater by calcined alkaline residue: batch and column studies, J. Taiwan Inst. Chem. Eng., 45 (2014) 1709–1716.
[34] J.P. Soetardji, J.C. Claudia, Y.-H. Ju, J.A. Hriljac, T.-Y. Chen, F.E. Soetaredjo, S.P. Santoso, A. Kurniawan, S. Ismadji, Ammonia removal from water using sodium hydroxide modified zeolite mordenite, RSC Adv., 5 (2015) 83689–83699.
[35] J. Wu, L. Jia, L. Wu, C. Long, W. Deng, Q. Zhang, Prediction of the breakthrough curves of VOC isothermal adsorption on hypercrosslinked polymeric adsorbents in a fixed bed, RSC Adv., 6 (2016) 28986–28993.
[36] Z.Z. Chowdhury, S.M. Zain, A.K. Rashid, R.F. Rafique, K. Khalid, Breakthrough curve analysis for column dynamics sorption of Mn(II) Ions from wastewater by using *Mangostana garcinia* peel-based granular-activated carbon, J. Chem., 2013 (2013) 8.
[37] T. Cheng, Y. Jiang, Y. Zhang, S. Liu, Prediction of breakthrough curves for adsorption on activated carbon fibers in a fixed bed, Carbon, 42 (2004) 3081–3085.
[38] R. Sabouni, H. Kazemian, S. Rohani, Mathematical modeling and experimental breakthrough curves of carbon dioxide adsorption on metal organic framework CPM-5, Environ. Sci. Technol., 47 (2013) 9372–9380.
[39] S.A. Ghorbanian, M. Davoudinejad, A. Khakpay, S. Radpour, Investigation of breakthrough curves of citric acid adsorption, Chem. Biochem. Eng. Q., 28 (2014) 329–336.
[40] M. Samarghandi, M. Hadi, G. McKay, Breakthrough curve analysis for fixed-bed adsorption of azo dyes using novel pine cone-derived active carbon, Adsorpt. Sci. Technol., 32 (2014) 791–806.
[41] W.T. Tsai, C.Y. Chang, C.Y. Ho, L.Y. Chen, Simplified description of adsorption breakthrough curves of 1,1-dichloro-1-fluoroethane (HCFC-141b) on activated carbon with temperature effect, J. Colloid Interface Sci., 214 (1999) 455–458.
[42] J.C. Moreno-Piraján, D. Rangel, B. Amaya, E.M. Vargas, L. Giraldo, Scale-up of pilot plant for adsortion of heavy metals, An. Asoc. Quim. Argent., 94 (2006) 71–82.
[43] M. Kukučka, N. Kukučka, A. Kukučka, A novel approach to adsorption kinetics calculation, Microporous Mesoporous Mater., 228 (2016) 123–131.
[44] J.K. Bediako, S. Kim, W. Wei, Y.-S. Yun, Adsorptive separation of Pb(II) and Cu(II) from aqueous solutions using as-prepared carboxymethylated waste Lyocell fiber, Int. J. Environ. Sci. Technol. (Tehran), 13 (2016) 875–886.
[45] M.A.S.D. Barros, P.A. Arroyo, E.A. Silva, General Aspects of Aqueous Sorption Process in Fixed Beds, 2013.
[46] N. Kukučka, Engineering Design of Nanofiltration Modules for the Reduction of Organic Matter and Arsenic from the Groundwater Aquifer, Environmental Engineering, PhD Thesis, 2013, p. 152.
[47] PuroTech Ltd., Installation, Operation & Maintenance Guide Crystal Right CR100 & CR200, pp. 1–16.
[48] Ž. Tomić, Possible application of synthetic zeolite CR-100 (Crystal-Right™) in ammonia adsorption from ground water of Banat aquifer, Eco-Energetic Engineering, 2016, p. 134.
[49] D.C. White, The Handbook of Chlorination and Alternative Disinfectants, Wiley-Interscience, New York, 1999.
[50] R. Perez-Garcia, P. Rodriguez-Benitez, Chloramine, a sneaky contaminant of dialysate, Nephrol. Dial. Transplant., 14 (1999) 2579–2582.
[51] R.W. Farmer, S.L. Kovacic, Catalytic activated carbon offers breakthrough for dialysis water treatment, Dial. Transplant., 26 (1997) 771–775.
[52] M. Kukučka, N. Kukučka, M. Vojinović-Miloradov, Ž. Tomić, M. Šiljeg, A novel approach to determine a resin's sorption characteristics for the removal of natural organic matter and arsenic from groundwater, Water Sci. Technol., 11 (2011) 726–736.
[53] Q. Deng, Ammonia Removal and Recovery from Wastewater Using Natural Zeolite: An Integrated System for Regeneration by Air Stripping Followed Ion Exchange, Master of Applied Science, 2014, p. 121.
[54] J.A. Lercher, A. Jentys, Handbook of Porous Solids, Wiley-VCH Verlag GmbH, 2008, pp. 1097–1156.
[55] M. Elanany, M. Koyama, M. Kubo, E. Broclawik, A. Miyamoto, Periodic density functional investigation of Lewis acid sites in zeolites: relative strength order as revealed from NH_3 adsorption, Appl. Surf. Sci., 246 (2005) 96–101.